Dynamic transitions in a three dimensional associating lattice gas model

Cite as: J. Chem. Phys. **132**, 134904 (2010); https://doi.org/10.1063/1.3354112
Submitted: 03 November 2009 . Accepted: 14 February 2010 . Published Online: 06 April 2010

Marcia M. Szortyka, Mauricio Girardi, Vera B. Henriques, and Marcia C. Barbosa

Dynamic transitions in a three dimensional associating lattice gas model

Marcia M. Szortyka,[1,a)] Mauricio Girardi,[2,b)] Vera B. Henriques,[3,c)] and Marcia C. Barbosa[1,d)]
[1]*Instituto de Física, Universidade Federal do Rio Grande do Sul, Caixa Postal 15051, Porto Alegre 91501-970, RS, Brazil*
[2]*Universidade Federal do Pampa, Caixa Postal 07, Bagé 96400-970, RS, Brazil*
[3]*Instituto de Física, Universidade de São Paulo, Caixa Postal 66318, São Paulo 05315-970, SP, Brazil*

(Received 3 November 2009; accepted 14 February 2010; published online 6 April 2010)

We investigate the thermodynamic and dynamic properties of a three dimensional associating lattice gas (ALG) model through Monte Carlo simulations. The ALG model combines a soft core potential and orientational degrees of freedom. The competition of directional attractive forces and the soft core potential results in two coexisting liquid phases which are also connected through order-disorder critical transitions. The model presents structural order, density, and diffusion anomalies. Our study suggests that the dynamic fragile-to-strong transitions are associated to changes in structural order. © *2010 American Institute of Physics*. [doi:10.1063/1.3354112]

I. INTRODUCTION

Water is the most important solvent in nature[1,2] presenting many unusual properties that are now well understood. However, an open question concerns the presence of a second critical point separating two liquid phases. It has been proposed some time ago that the anomalous behavior of water might be associated with a critical point at the terminus of a liquid-liquid coexistence line, localized in the unstable supercooled liquid region,[3] at high pressures. In spite of the limit of 235 K below where water cannot be found in the liquid phase without crystallization, two amorphous phases were observed at much lower temperatures.[4] There are evidences, although yet under test, that these two amorphous phases are related to fluid water.[5,6]

More recently, experimental studies have shown that water presents anomalies also for dynamic properties. Results in nanoscale hydrophilic pores show a line of dynamic crossover in water diffusivity in the pressure-temperature phase diagram.[7–10] At constant pressure, as the temperature is lowered, a fragile-to-strong crossover is observed in the diffusivity.[7–10] This line coincides with the line of peaks in the specific heat suggesting that it is a Widom line (WL). This line is defined as the analytic continuation of the coexistence line between two phases ending in a critical point. Along a WL the specific heat does not diverge but has a peak that becomes larger as the critical point is approached. Consequently the dynamic transitions observed in the experiments were interpreted in terms of the liquid-liquid phase transition predicted in water.[9] The authors propose that the presence of fragile-to-strong transition in a region that does exhibit density anomaly indicates the presence of a liquid-liquid transition.

Waterlike anomalous properties are also present in the behavior of other substances. The dynamic transition has also been associated with the first-order liquid-liquid transition in silicon[11] instead of being at the WL as suggested for water.[9] In addition, the fragile-to-strong crossover has also been observed in silica and related to the polyamorphic behavior of amorphous silica and to the presence of two liquid phases. No thermodynamic transition is observed in this case.[12]

The discovery of anomalous dynamic properties has posed new questions in relation to polymorphism. Is there a relation between the fragile-to-strong crossover and the presence of liquid-liquid transitions? What is the nature of the liquid-liquid transitions? What is the role of structural order in relation to thermodynamic or dynamic anomalies?[13] Here we address these questions by studying the associating lattice gas model that exhibits two liquid phases and different ordered phases. This waterlike model has density and diffusion anomalies[14,15] and its phase diagram has been investigated previously through Monte Carlo simulations[14] and cluster expansions.[16]

In the numerical study of the model by Girardi *et al.*[14,15] two coexisting liquid phases, as well as density and diffusion anomalies were found. Buzano *et al.*[16] explored the same model by an analytical method. Their calculations yielded an additional critical line connecting the two coexistence lines, as well as a second critical line between the liquid phase and the high temperature fluid phase, not foreseen in the numerical study. This last line, according to their analysis, ends at the liquid-gas coexistence phase boundary at a critical end point.

Here we explore the model phase diagram through Monte Carlo simulations in order to check for the effect of fluctuations not included in the approach by Buzano *et al.*[16] We then address the question on the behavior of the diffusivity in the vicinity of the critical regions.

The remaining of the paper goes as follows. In Sec. II the model is introduced and the employed Monte Carlo simulations are described. In Sec. III the chemical potential

[a)]Electronic mail: marcia.szortyka@ufrgs.br.
[b)]Electronic mail: mauricio.girardi@unipampa.edu.br.
[c)]Electronic mail: vhenriques@if.usp.br.
[d)]Electronic mail: marcia.barbosa@ufrgs.br.

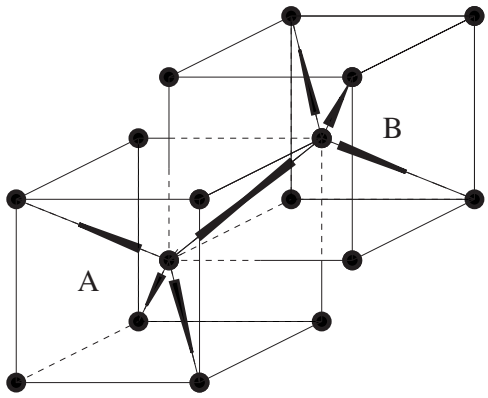

FIG. 1. Particles in the bcc lattice can assume arm configurations A or B.

versus temperature phase diagram obtained by Monte Carlo simulations is presented. In Sec. IV the behavior of the diffusion coefficient across the critical lines and the first-order liquid-gas coexistence line are analyzed. Final comments are presented in Sec. V.

II. THE MODEL

We consider the three dimensional associating lattice gas model of $V=L^3$ sites on a body centered cubic (bcc) lattice, as introduced by Girardi *et al.*[14] Some aspects of the phase diagram were previously described by Monte Carlo[14] and by analytical methods.[16] Particles are represented by an occupational variable σ_i, with $\sigma_i=0$ if the site is empty or $\sigma_i=1$ if the site is occupied by a molecule. In addition, each particle has eight arm variables τ_i that represent the possibility of forming a bond with a neighbor site. Four arms are the usual ice bonding arms with $\tau_i=1$, the other four are inert with $\tau_i=0$. The bonding and nonbonding arms are distributed in a tetrahedral arrangement imposed by the lattice geometry. The two possible arm configurations, A and B, are illustrated in Fig. 1.

The system is described by the Hamiltonian

$$\mathcal{H}=\sum_{\langle i,j\rangle}\sigma_i\sigma_j(\epsilon+\gamma\tau_i\tau_j), \tag{1}$$

where $\sigma_i=0,1$ is the occupational variable, ϵ is the van der Waals energy, γ is the bond energy, and $\tau_i=0,1$ is the arm variable that represents the possibility of a bond between two neighboring sites. A bond is formed when two neighboring sites have bonding arms variables equal to 1, $\tau_i\tau_j=1$. The parameters are chosen to be $\epsilon>0$ and $\gamma<0$, which implies in an energetic penalty to the neighbors that do not form a bond.

The ground state properties of the model were obtained by inspecting Eq. (1) with an external chemical potential term. The grand potential per site, at zero temperature, is given by $\phi=e-\mu\rho$, where $\phi=\Phi/V$, $e=\mathcal{H}/V$, N is the number of occupied sites, and $\rho=N/V$ is the density of the system. For chemical potentials lower than $\mu<2(\epsilon+\gamma)$ the system is in the gas phase, where the lattice is empty ($\rho=0$). At chemical potential $\mu_c=2(\epsilon+\gamma)$ the gas phase coexists with the low density liquid (LDL) phase with $\rho=0.5$. This phase is present in the chemical potential range $2(\epsilon+\gamma)<\mu<6\epsilon+2\gamma$. In the LDL phase each particle has four occupied neighboring sites with which bonds are formed as illustrated in Fig. 2. At the chemical potential $\mu_c=6\epsilon+2\gamma$ the LDL phase coexists with a high density liquid (HDL) phase, with $\rho=1$. This phase is present for chemical potentials higher than $\mu>6\epsilon+2\gamma$. In this phase all sites are occupied and each molecule forms four bonds, as can be seen in Fig. 3. Here, molecules have first neighboring sites with no bond formed. The chemical potential is so high that it compensates the penalty imposed by occupation of sites with no bond.

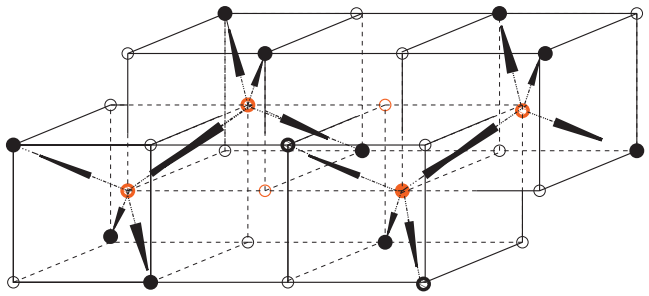

FIG. 2. In the ordered LDL phase half of the lattice is occupied by particles.

The nonzero temperature properties of the model were obtained by Monte Carlo simulations in the grand canonical ensemble with the METROPOLIS algorithm, for lattices with linear size $L=30$ and interaction parameter $\gamma/\epsilon=-2$. Reduced parameters were defined as

$$\bar{T}=\frac{k_BT}{\epsilon},$$
$$\bar{\mu}=\frac{\mu}{\epsilon}. \tag{2}$$

The stability of the solutions were tested from comparison of results for lattices of linear sizes $L=20,30,40,50$, as shown in the next section. Since no qualitative changes occurred in the model properties, we chose lattice size $L=30$ for an extensive study.

III. THE PHASE DIAGRAM

The complete chemical potential versus temperature phase diagram in reduced units, obtained by Monte Carlo simulations, is illustrated in Fig. 4. We observed that the gas phase coexists with the LDL phase in a first order transition line (solid line and circles) that ends at the point ($\bar{T}_{c_1}=1.39$, $\bar{\mu}_{c_1}=0.09$). The LDL phase coexists with the HDL

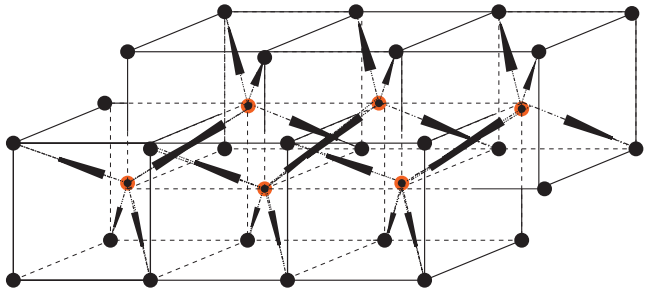

FIG. 3. In the ordered HDL phase the lattice is fully occupied by particles.

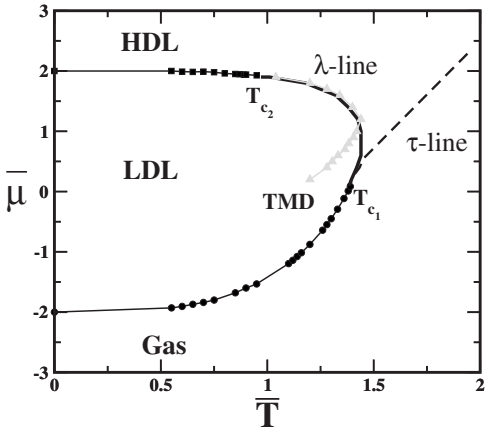

FIG. 4. Chemical potential vs temperature phase diagram in reduced units. Solid line and circles are the coexistence line between gas-LDL, while solid line and squares is the coexistence line between LDL-HDL. T_{c_1} point is a bicritical point from where the critical λ-line and τ-line emanate. T_{c_2} point is a tricritical point where the λ-line joins to the LDL-HDL coexistence line.

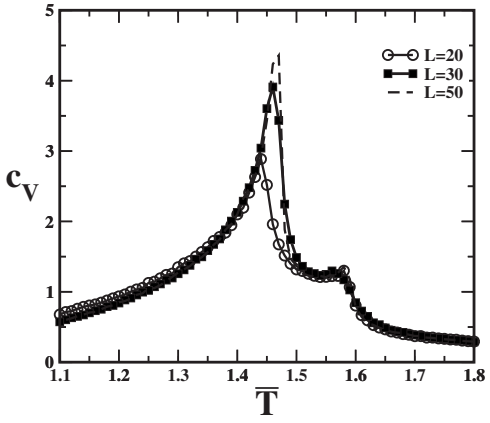

FIG. 5. Specific heat at constant volume, c_V, vs reduced temperature for reduced chemical potential $\bar{\mu}=1$ and lattice sizes $L=20$, 30, and 50.

phase in a first order transition line (solid line and squares) that ends at the point ($\bar{T}_{c_2}=0.95$, $\bar{\mu}_{c_2}=1.93$). This system exhibits a region of anomalous density as observed by Monte Carlo simulations by Girardi *et al.*[14] and by cluster variational methods by Buzano *et al.*[16] The line of temperature of maximum density (TMD) is located between the two coexistence lines and is represented by a gray solid line and triangles in Fig. 4. Both the LDL and the HDL are fluid phases because the diffusion coefficient is nonzero in both cases.

From the point T_{c_1} two lines appear, the λ-line (solid line) and the τ-line (dashed line). The λ-line starts at the point T_{c_1}, joins the gas-LDL and LDL-HDL coexistence lines, ending at the T_{c_2} point. This line has a re-entrant format similar to the phase boundaries observed in liquid-solid transitions in models with two length scales.[17] The τ-line starts at the point T_{c_1} and extends itself in the high temperature and chemical potential region of the phase diagram. Differently from the mean-fieldlike results of Buzano *et al.*[16] the τ line does not end at a critical end point on the liquid-gas coexistence curve. In our investigation of the model through numerical simulations, the LDL-gas coexistence line ends at a bicritical point. This change is certainly due to the fluctuations missed in their approach.

In order to define the character of these two lines, the specific heat at constant volume, defined by the equation[18]

$$c_V = \frac{1}{k_B T^2 V}\left(\langle \delta\phi^2\rangle_{\mu VT} - \frac{\langle \delta\phi\delta\rho\rangle^2_{\mu VT}}{\langle \delta\rho^2\rangle_{\mu VT}}\right) \tag{3}$$

was computed. Here $\delta Z = Z - \langle Z\rangle$ with $Z=\phi,\rho$.

The behavior of c_V with reduced temperature is shown in Fig. 5 for reduced chemical potential $\bar{\mu}=1$ and different lattice sizes. For this chemical potential, the specific heat presents two different peaks, suggesting the presence of a double criticality. For a lattice size $L=30$, the first peak is located at $\bar{T}\simeq 1.44$, the location of the λ-line, and the second one at $\bar{T}\simeq 1.58$, the location of the τ-line. By varying the chemical potential, the two peaks in the specific heat are present in the interval $\mu_{T_{c_1}} < \mu < \mu_{T_{c_2}}$ and the λ and the τ lines can be located for different chemical potentials.

The criticality of both λ and τ lines was confirmed by computing the fourth-order cumulant of energy, given by

$$V_L = 1 - \frac{\langle (\mathcal{H} - \langle \mathcal{H}\rangle)^4\rangle}{3\langle (\mathcal{H} - \langle \mathcal{H}\rangle)^2\rangle^2}. \tag{4}$$

The result is shown in Fig. 6 for reduced chemical potential $\bar{\mu}=1$ and lattice sizes $L=20$, 30, and 50. The behavior of V_L with temperature and lattice size tell us that both lines are critical and of second order.[19] In order to check the nature of the criticality of the λ and τ lines, the order of both particle orientation and lattice occupation was inspected.

Particle arm configurations allow for two particle orientational states (see Fig. 1), which we designed as A and B, and describe through variables $S_i=1$ and $S_i=-1$. Inspection of particle orientation both in the ordered LDL as well as in the ordered HDL phase suggests (see Figs. 2 and 3) the division of the lattice into two sublattices, illustrated in Fig. 7. Then a possible orientational bonding order parameter may be defined as

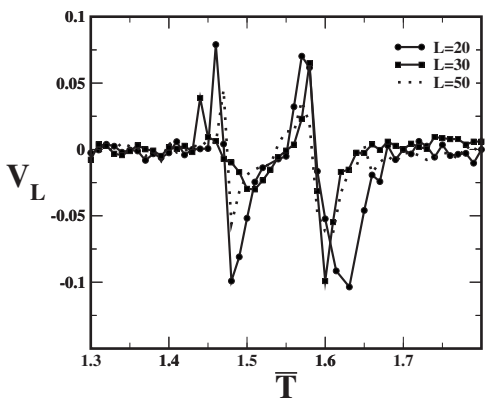

FIG. 6. Cumulant of energy vs reduced temperature for reduced chemical potential $\bar{\mu}=1$ and lattice sizes $L=20$, 30, and 50.

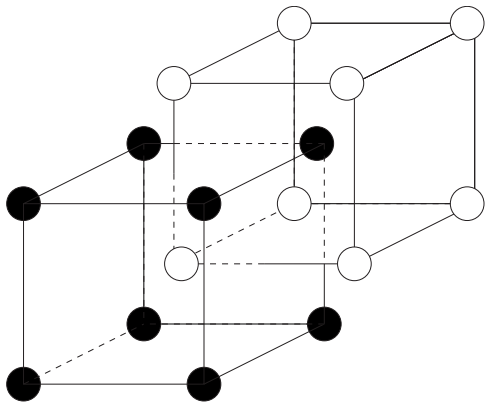

FIG. 7. The lattice is divided in two sublattices: Full circles define sublattice 1 while empty circles define sublattice 2.

$$\theta_{\text{bond}_X} = \frac{|\langle S_i \rangle|_X}{N_X}, \tag{5}$$

where $X=1,2$ is the sublattice index and N_X is the number of particles in sublattice X. $\theta_{\text{bond}} \neq 0$ if there is predominance of a particular molecular orientation on sublattice X.

Behavior of θ_{bond} is illustrated in Fig. 8 for reduced chemical potential $\bar{\mu}=1$ and lattice size $L=30$. It can be seen that when the critical τ-line is crossed the system starts to order itself by increasing abruptly the number of particles in the same arm configuration. Particles that belongs to sublattice 1 are predominantly in arm configuration A, while particles that belong to sublattice 2 are mostly in arm configuration B.

A fully tetrahedral network develops on crossing the second critical λ-line, at which the system releases unbounded particles on half of the lattice. This can be better visualized by dividing the lattice into eight sublattices, as illustrated in Fig. 9, and measuring density of particles ρ_i and density of bonds ρ_{b_i}, with $i=1,\ldots,8$. ρ_i is the density of the sublattice i while ρ_{b_i} is the number of bonds divided by the number of sites in the sublattice i. At the λ-line four sublattices become empty while other four become full, as illustrated in Fig. 10(a) by the behavior of ρ_i with temperature. A translational order parameter may be defined as $\theta_{tr}=\rho_1-\rho_2$, where ρ_1 is the density of particles of the one of the sublattices, 1, 4, 6, 7, and ρ_2 the density of particles of sublattices 2, 3, 5, and 8 as illustrated in Fig. 9.

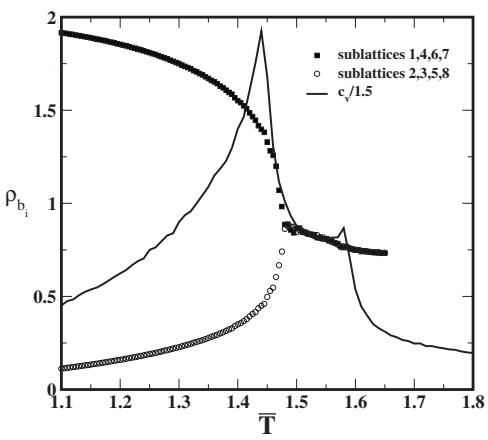

FIG. 8. Order parameter and specific heat vs temperature for chemical potential $\bar{\mu}=1$ and lattice size $L=30$. As can be seen, both sublattices order themselves in one arm configuration when crossing the τ-line.

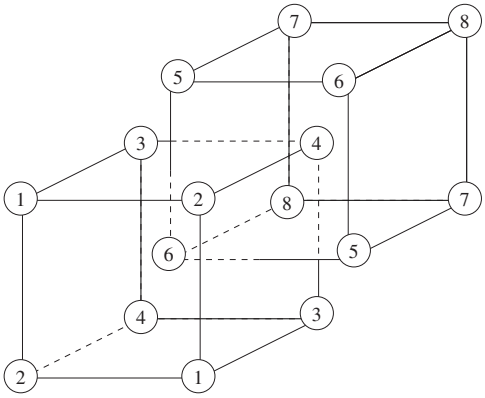

FIG. 9. The eight sublattices division. Sublattices 1, 4, 6, and 7 become occupied, while the other sublattices become empty. Particles on sublattices 1 and 4 orient mostly in the A state, while particles on sublattices 6 and 7 orient into the B state.

Translational order is accompanied by establishment of a bonding network, as illustrated in Fig. 10(b) by the behavior of ρ_{b_i} with temperature. Thus, the abrupt increase in orientational order at the τ-line is not complete (see Fig. 8) and bonding is relatively low in the HDL phase [see Fig. 10(a)].

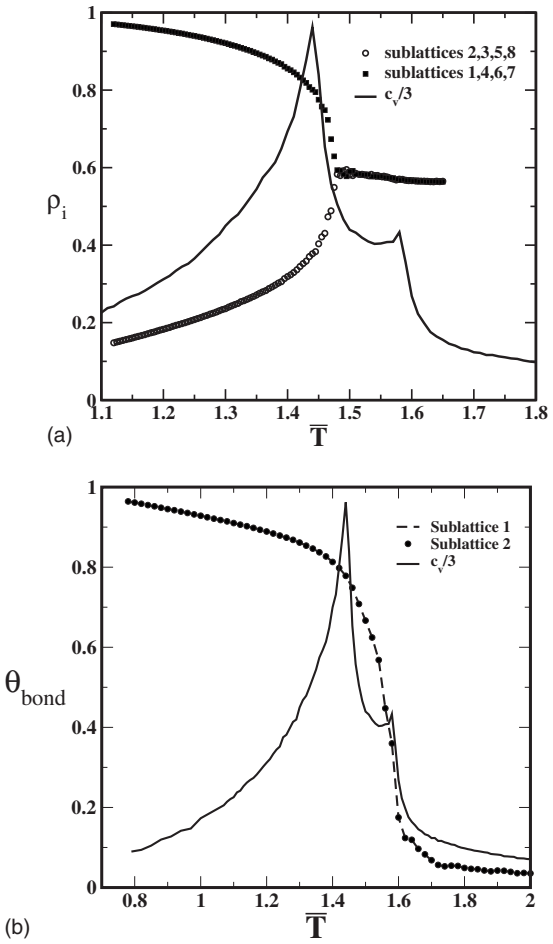

FIG. 10. Density of particles and density of bonds of each sublattice vs reduced temperature.

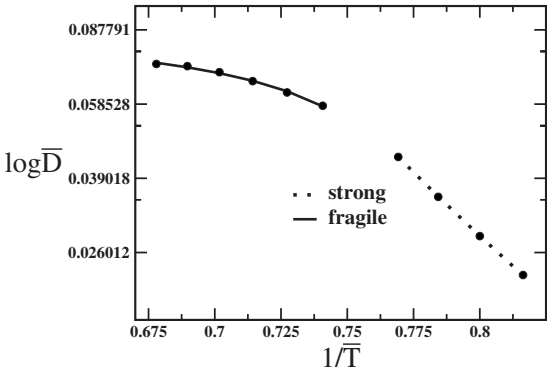

FIG. 11. Diffusion coefficient in an Arrhenius plot for $\bar{\mu}=0$. At high temperatures, diffusivity follows a non-Arrhenius law, while at low temperatures diffusivity follows an Arrhenius law. The dynamic crossover takes place when the system crosses the coexistence line between the gas-LDL phases.

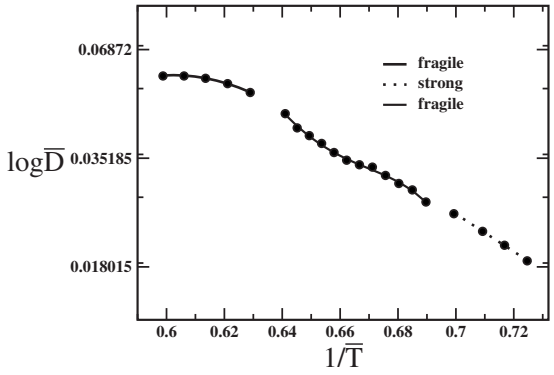

FIG. 12. Diffusion coefficient as a function of temperature in an Arrhenius plot for $\bar{\mu}=1.0$. For temperatures $T>T_\tau$ diffusivity follows a non-Arrhenius law, characterizing the liquid as fragile. At temperatures $T_\lambda<T<T_\tau$, the liquid is also characterized as fragile since diffusivity follows a non-Arrhenius law. For temperatures $T<T_\lambda$ diffusivity follows an Arrhenius law, and the liquid is characterized as strong.

In summary as the temperature lowers at constant chemical potential, the system first orders orientationally, at the τ-line, at which predominance of one of the orientational states in each sublattice arises ($\theta_{\text{bond}}\neq 0$) and then orders positionally, with the lattice becoming half empty at the λ-line. Simultaneous orientational and positional order is accompanied by the development of a fully developed bond network. Figure 4 shows two critical lines not present in the previous analysis shown in Refs. 14 and 15.

IV. DYNAMIC TRANSITIONS

The behavior of the diffusion coefficient was analyzed as a function of the temperature for chemical potential $\bar{\mu}=0$, crossing the first-order gas-LDL coexistence line, and $\bar{\mu}=1$, crossing the critical λ and τ lines.

To compute diffusion coefficient the system is equilibrated at fixed chemical potential and temperature. In equilibrium this system has n particles. Starting from this equilibrium configuration at a time $t=0$, each one of the n particles is allowed to move to an empty randomly chosen neighbor site. The movement is accepted if the total energy of the system is reduced, otherwise it is accepted with a probability $\exp(\Delta E/k_BT)$ where ΔE is the difference between the energy of the system after and before the movement. After repeating this procedure nt times, the mean square displacement per particle at a time t is given by

$$\langle(\Delta\bar{\mathbf{r}}(t))^2\rangle=\langle(\bar{\mathbf{r}}(t)-\bar{\mathbf{r}}(0))^2\rangle, \tag{6}$$

where $\bar{\mathbf{r}}(t)=\mathbf{r}(t)/a$ is the particle's position measured in units of lattice parameter a, $\bar{\mathbf{r}}(0)$ is particle's position at the initial time, and $\bar{\mathbf{r}}(t)$ is the particle's position at a time t. In Eq. (6), the average is taken over all particles and over different initial configurations. The dimensionless diffusion coefficient is then obtained from Einstein's relation

$$\bar{D}=\lim_{t\to\infty}\frac{\langle(\Delta\bar{r}(t))^2\rangle}{6t} \tag{7}$$

with time measured in units of Monte Carlo steps.

First, let us examine the behavior of diffusivity when the system crosses the gas-LDL first-order coexistence line. Figure 11 shows the logarithm of diffusion coefficient versus the inverse of temperature for chemical potential $\bar{\mu}=0$. At high temperatures diffusivity follows a non-Arrhenius trend namely

$$\bar{D}=A_0+A_1\bar{T}+A_2\bar{T}^2+A_3\bar{T}^3 \tag{8}$$

indicating that the low density disordered fluid phase is a fragile liquid. At low temperatures, below the gas-LDL transition temperature, diffusivity displays an Arrhenius behavior, given by

$$\bar{D}=B_0\exp\left(\frac{B_1}{\bar{T}}\right) \tag{9}$$

characterizing the LDL phase as a strong liquid. In both equations A_i and B_i are the fitting parameters. In conclusion, the system undergoes a fragile-to-strong transition when crossing the gas-LDL coexistence line at constant chemical potential. This result indicates that the more ordered structure (LDL) exhibits a strong liquid behavior.

Next, we describe what happens with diffusivity behavior when the system crosses each one of the two critical lines. Figure 12 shows the logarithm of diffusion coefficient as a function of the inverse of temperature for chemical potential $\bar{\mu}=1.0$. At very high temperatures, for $\bar{T}>1.58$, or $1/\bar{T}<0.63$, diffusivity displays a non-Arrhenius behavior, given by Eq. (8).

Lowering the temperature, when the system crosses critical τ-line, in the temperature range $0.64<1/\bar{T}<0.69$ between the two critical lines, the liquid also exhibits a fragile behavior, were diffusion coefficient follows a non-Arrhenius trend given by Eq. (8) with a different set of fitting parameters than the previous case. For even low temperatures the system crosses the λ-line, and for $1/\bar{T}>0.70$ diffusivity follows an Arrhenius law given by Eq. (9) characterizing the liquid as strong.

The results show that the system undergoes a fragile-strong crossover when crosses the first-order gas-LDL coexistence line (coming from high temperatures), a fragile-fragile crossover when crosses the critical-τ line (coming

from high temperatures) and a fragile-strong crossover when crosses the critical λ-line (also coming from high temperatures).

V. FINAL COMMENTS

In this paper we have analyzed the thermodynamic and dynamical properties of a three dimensional associating lattice gas model. The system presents two liquid phases which coexist through first order lines at low temperatures. At low density and temperature, the system presents an open four-bonded orientational structure. As chemical potential is raised, the system undergoes a transition to a HDL, as the lattice is filled up, loosing translational order. At very low chemical potential, the LDL coexists with a gas phase. At higher temperatures, the two coexistence lines are linked by a critical line which we have called the λ-line. Thus the coexistence line between the HDL and the LDL phases ends at a tricritical point from which the λ-line emerges. A second critical line, the τ-line, emerges from the LDL-gas coexistence line which ends at a bicritical point. The criticality of both lines is identified from the specific heat study as well as from the cumulant of energy. Our model has some resemblance with other lattice models in two[20–23] and three dimensions[16,24,25] that exhibit two liquid phases.

We propose the characterization of the different liquid phases in terms of structural order through positional and orientational order parameters. In the LDL phase, a tetrahedral bond network is present: The system presents both translational an orientational order. As temperature is lowered from the fluid phase, at intermediate chemical potentials, the system undergoes two phase transitions. At the first one, at which the HDL phase is reached, orientational order of particles on different sublattices rises abruptly. The second transition leads to the LDL phase, at which the system orders also translationally, with some of the sublattices becoming empty, while others fill up. Thus the two liquid phases coexist at low temperatures, with different densities, while at higher temperatures they are separated by order-disorder transitions. The line of maximum densities (TMD) is located inside the structurally ordered phase.

The thermodynamic phase transitions are accompanied by dynamic transitions, baring no relation to a WL. Our results point to a connection between strong-to-fragile transitions and order-disorder transitions, as suggested by Angell.[26] At lower chemical potentials the system exhibits a fragile-to-strong transition at the gas-LDL coexistence line. The fragile-to-strong transition occurs simultaneously with an ordering transition to the tetrahedrally bonded LDL phase. At higher chemical potentials, the system undergoes two dynamic transitions connected to the two critical order-disorder transitions. As temperature is lowered and the orientational order-disorder τ-line is reached, the system exhibits a fragile-to-fragile transition. As temperature is further decreases, a fragile-to-strong transition accompanies the translational order-disorder λ-line transition which yields the tetrahedrally bonded network of the LDL phase.

The presence of the fragile-to-strong transition at the order-disorder critical line was also observed in the two dimensional version of this model[27] and in Ref. 22, confirming the assumption that the change in the structure is fundamental to determine the non-Arrhenius to Arrhenius behavior.

ACKNOWLEDGMENTS

This work is partially supported by CNPq, INCT-FCx.

[1] G. W. Robinson, S.-B. Zhu, S. Singh, and M. W. Evans, *Water in Biology, Chemistry, and Physics: Experimental Overviews and Computational Methodologies*, (World Scientific, Singapore, 1996).
[2] M.-C. Bellissent-Funel, *Hydration Processes in Biology: Theoretical and Experimental Approaches* (IOP, Amsterdam, 1999).
[3] P. H. Poole, F. Sciortino, U. Essmann, and H. E. Stanley, Nature (London) **360**, 324 (1992).
[4] O. Mishima, L. D. Calvert, and E. Whalley, Nature (London) **310**, 393 (1984).
[5] R. S. Smith and B. D. Kay, Nature (London) **398**, 302 (1999).
[6] O. Mishima and Y. Suzuki, Nature (London) **419**, 599 (2002).
[7] A. Faraone, L. Liu, C.-Y. Mou, C.-W. Yen, and S.-H. Chen, J. Chem. Phys. **121**, 10843 (2004).
[8] L. Liu, S.-H. Chen, A. Faraone, S.-W. Yen, and C.-Y. Mou, Phys. Rev. Lett. **95**, 117802 (2005).
[9] L. Xu, P. Kumar, S. V. Buldyrev, S.-H. Chen, P. Poole, F. Sciortino, and H. E. Stanley, Proc. Natl. Acad. Sci. U.S.A. **102**, 16558 (2005).
[10] S.-H. Chen F. Mallamace, C-.Y. Mou, M. Broccio, C. Corsaro, A. Faraone, and L. Liu, Proc. Natl. Acad. Sci. U.S.A. **103**, 12974 (2006).
[11] S. Sastry and C. A. Angell, Nature Mater. **2**, 739 (2003).
[12] I. Saika-Voivod, P. Poole, and F. Sciortino, Nature (London) **412**, 514 (2001).
[13] J. R. Errington and P. G. Debenedetti, Nature (London) **409**, 318 (2001).
[14] M. Girardi, A. L. Balladares, V. Henriques, and M. C. Barbosa, J. Chem. Phys., **126**, 064503 (2007).
[15] M. Girardi, M. Szortyka, and M. C. Barbosa, Physica A **386**, 692 (2007).
[16] C. Buzano, E. De Stefanis, and M. Pretti, J. Chem. Phys. **129**, 024506 (2008).
[17] N. G. Almarza, J. A. Capitan, J. A. Cuesta, and E. Lomba, J. Chem. Phys. **131**, 124506 (2009).
[18] M. P. Allen and D. J. Tildesley, *Computer Simulations of Liquids* (Clarendon, Oxford, 1987).
[19] S.-H. Tsai and S. R. Salinas, Braz. J. Phys. **28**, 58 (1998).
[20] C. Buzano, E. De Stefanis, A. Pelizzola, and M. Pretti, Phys. Rev. E **69**, 061502 (2004).
[21] V. B. Henriques and M. C. Barbosa, Phys. Rev. E **71**, 031504 (2005).
[22] P. Kumar, G. Franzese, and H. E. Stanley, Phys. Rev. Lett. **100**, 105701 (2008).
[23] C. E. Fiore, M. M. Szortyka, M. C. Barbosa, and V. B. Henriques, J. Chem. Phys. **131**, 164506 (2009).
[24] C. J. Roberts and P. G. Debenedetti, J. Chem. Phys. **105**, 658 (1996).
[25] M. Pretti and C. Buzano, J. Chem. Phys. **121**, 11856 (2004).
[26] C. A. Angell, J. Phys.: Condens. Matter **19**, 205112 (2007).
[27] M. M. Szortyka, M. Girardi, V. B. Henriques, and M. C. Barbosa, J. Chem. Phys. **130**, 184902 (2009).